

# Turn-Aware LSTM Model for Vehicle Trajectory Forecasting

X. Zhou<sup>1</sup> C. Alecsandru<sup>2</sup> S. Bashbaghi<sup>3</sup> Y. Jeong<sup>1</sup> Y. Chen<sup>1</sup>

<sup>1</sup> Department of Engineering, Concordia University, Montreal, Canada

<sup>2</sup> Associate Professor at Concordia University, Montreal, Canada

<sup>3</sup> Senior Data Scientist, Ericsson, Montreal, Canada

email: xingnan.zhou@mail.concordia.ca; ciprian.alecsandru@concordia.ca;  
saman.bashbaghi@ericsson.com; hziyeong@gmail.com; ye.chen@mail.concordia.ca

---

## Abstract

Accurate trajectory prediction is essential for autonomous driving safety at intersections. Existing deep learning models often overlook turning behaviors, leading to curvature misestimation. This study proposes a Turn-Aware LSTM network that explicitly encodes maneuver intentions—left, right, or straight—using vehicle trajectories extracted from UAV footage via YOLOv8 and DeepSORT. To mitigate tracking noise, a cumulative turning-angle strategy is introduced for robust maneuver classification. Experiments demonstrate that the proposed model significantly improves prediction accuracy for turning maneuvers, reducing Final Displacement Error (FDE) by 15–20% at a 3-second horizon compared to vanilla LSTM and physics-based baselines. The findings validate the integration of maneuver-aware encoding for enhanced intersection-level forecasting in real-time applications

*Keywords – Vehicle trajectory prediction, LSTM, Spatiotemporal relationship, Turning behavior, Encoding*

---

## 1. Introduction

30 The coexistence of Connected Autonomous Vehicles (CAVs) and Conventional Vehicles  
31 (CONVs) on urban roads poses significant challenges to traffic safety and efficiency [1]. One of  
32 the key components for addressing these challenges is trajectory forecasting, which enables  
33 autonomous vehicles to anticipate potential conflicts and make informed decisions to enhance  
34 traffic flow and safety [2]. However, many existing trajectory prediction approaches heavily rely  
35 on external data sources, such as GPS signals and detailed road geometry, which inherently limits  
36 their scalability and adaptability [3]. Given the complexity of urban traffic networks, a solution  
37 that

38 uses only vehicle trajectory data to infer lane positions and turning behaviors is essential for  
39 real-world deployment and effective decision-making.

40 Previous studies on Vehicle Trajectory Prediction (VTP) have explored various deep learning-  
41 based approaches to improve accuracy. Notably, models such as STA-LSTM, which integrates  
42 spatial-temporal attention mechanisms, have enhanced the interpretability of vehicle trajectory  
43 predictions by incorporating historical trajectory patterns and interactions with neighboring  
44 vehicles [4]. Another promising approach is the Graph Attention Network (GAT) combined with  
45 LSTM encoders, which encodes motion data and inter-vehicle relationships to generate robust  
46 trajectory forecasts [5]. These approaches have advanced the field, but their predictive accuracy  
47 remains limited in urban intersections where vehicles frequently execute left turns, right turns, or  
48 lane changes. Most models still rely on position-only trajectory data without explicitly encoding  
49 lane-level context or maneuver intentions, leading to degraded performance precisely when  
50 turning behavior drives safety-critical outcomes.

51 In mixed-traffic environments of connected/autonomous vehicles (CAVs) and conventional  
52 vehicles (ConVs), accurate forecasting becomes even more important. Autonomous vehicles must  
53 anticipate turning and lane-changing maneuvers at intersections and freeway exits to avoid  
54 conflicts, yet conventional LSTM-based models—often trained on datasets such as NGSIM—are  
55 constrained by fixed-camera viewpoints, occlusion, and limited spatial resolution. These  
56 shortcomings reduce their ability to learn lane-specific functions and robustly recognize turning  
57 intent, weakening their practical applicability in real-world traffic management [5].

58 To address these limitations, this study proposes a Turn-Aware LSTM that explicitly  
59 integrates maneuver features—left turns, right turns, and straight-through movements—into an  
60 encoder–decoder forecasting framework. By encoding turning intent alongside kinematic states,  
61 the model reduces errors that typically occur during turning maneuvers, while maintaining  
62 accuracy for straight trajectories. Importantly, this work leverages high-resolution UAV-captured  
63 traffic data, which offers wide spatial coverage and minimizes occlusion compared to fixed-  
64 camera datasets. The richer, more continuous data stream enables more reliable labeling of  
65 turning behaviors and provides a realistic foundation for training and testing the proposed model.

66 Building on the above, we summarize our contributions as follows.

67 (i) It shows that explicit maneuver encoding—implemented via a 1-s cumulative heading  
68 change and one-hot turn indicators—stabilizes maneuver recognition and yields targeted accuracy  
69 gains where prediction is hardest: left and right turns. Improvements are concentrated on turning  
70 ADE/FDE while leaving straight-through performance essentially unchanged.

71 (ii) It presents a Turn-Aware LSTM that augments a standard encoder–decoder with turn  
72 features on the input side. The model is lightweight ( $\approx 2\text{--}3$  ms per vehicle on an RTX 4090),  
73 matching vanilla-LSTM latency and thus suitable for real-time use.

(iii) It provides maneuver-resolved evaluations across 1–3 s horizons against CV, vanilla LSTM, and a Tiny Transformer. While the Transformer attains the lowest overall errors, the Turn-Aware LSTM consistently outperforms the vanilla LSTM—most notably for 3-s turning forecasts (~15–20% FDE reduction)—thereby isolating the benefit of maneuver encoding. The dataset, preprocessing pipeline, and threshold sensitivity (5°/10°/15°) are documented for reproducibility, and we discuss generalization beyond the study site as well as extensions to LiDAR/V2X fusion and turn-aware Transformer/GNN variants.

The remainder of this paper is structured as follows: Section 2 reviews existing trajectory prediction approaches, with particular attention to their limitations in handling turning maneuvers and intersection scenarios, thereby motivating the need for maneuver-aware forecasting models in this study. Section 3 details the research methodology, including UAV-based data collection at a signalized intersection, preprocessing techniques for stabilizing trajectories and encoding turning behaviors, and the design of the proposed Turn-Aware LSTM architecture. Section 4 reports the experimental results and comparative analysis, highlighting how maneuver-aware encoding improves prediction accuracy over baseline models and discussing challenges such as noise, stationarity, and long-horizon drift. Finally, Section 5 concludes the paper by summarizing key contributions, outlining implications for autonomous driving and traffic management, and suggesting directions for broader validation and multimodal extensions.

## 2. Literature Review

Vehicle behaviour detection is essential for traffic monitoring research, with most existing methods relying on vehicle trajectory analysis. Traditional machine learning techniques, such as Fuzzy C-Means (FCM) and Support Vector Machines (SVM), have been employed to classify vehicle trajectories. Saini et al. demonstrated the effectiveness of FCM and SVM in trajectory classification, although these methods exhibited limitations in feature robustness[6]. Similarly, Yao et al. [7] proposed a trajectory clustering framework that encodes trajectory depth as a fixed-length feature sequence, while Choong et al. [8] utilized the Longest Common Subsequence (LCSS) algorithm to measure trajectory similarity before clustering. Despite their contributions, these traditional methods struggle to scale effectively for large datasets and dynamic traffic conditions, limiting their applicability in real-world traffic analysis.

Deep learning models, particularly Long Short-Term Memory (LSTM) networks, have gained significant traction in vehicle behaviour detection due to their capability to handle sequential data and address vanishing gradient issues [9]. LSTMs have been successfully applied in behaviour recognition, including robot behaviour classification and abnormal behaviour detection in video sequences [10]. In the context of vehicle trajectory prediction, Morton et al. [11] utilized LSTMs to predict vehicle acceleration on highways, demonstrating superiority over traditional models. Further improvements were introduced by Ding et al. [12], who combined LSTM-based models with Convolutional Neural Networks (CNNs) to detect unsafe driving behaviours. These studies highlight the effectiveness of LSTM-based approaches for trajectory prediction but also expose the limitations of current models in capturing complex spatial-temporal dependencies, particularly in mixed-traffic environments.

To address the challenge of modelling interactions between multiple vehicles, researchers have integrated attention mechanisms and graph-based models into LSTM architectures. The Spatiotemporal Attention Long Short-Term Memory (STA-LSTM) model, introduced by Lei Lin et al. [4], incorporates spatial-temporal attention mechanisms to enhance vehicle trajectory

120 prediction by identifying how historical trajectories and surrounding vehicles influence future  
121 movement. Similarly, Yang and Pei [13] developed the Long-Short Term Spatio-Temporal  
122 Aggregation (LSSTA) network, which combines transformer networks with Temporal  
123 Convolution Networks (TCN) to improve long-term dependency modelling in vehicle behaviour  
124 prediction. Despite these advances, many models continue to depend on external data sources,  
125 such as GPS and road geometry, making them less adaptable to real-world scenarios.

126 Our study introduces a Turn-Aware LSTM model that exclusively relies on vehicle trajectory  
127 data to identify lane positions and predict turning behaviours, eliminating the need for GPS or  
128 road geometry inputs. This approach directly addresses the limitations in existing research by  
129 emphasizing lane-specific interactions and turning behaviours to improve trajectory prediction  
130 accuracy. The customized YOLOv8 model was trained on high-resolution drone footage collected  
131 at intersections, allowing for enhanced vehicle detection and tracking [14]. By analysing  
132 cumulative directional changes and displacement patterns, our model classifies turning behaviours  
133 based on angular variations, providing a robust framework for real-time vehicle behaviour  
134 prediction.

135 The reliance on fixed roadside cameras, such as those used in the NGSIM dataset [15], has  
136 posed challenges for vehicle trajectory prediction due to occlusions, limited spatial resolution, and  
137 constrained fields of view. These limitations can lead to incomplete or inaccurate vehicle  
138 detection, particularly in high-density traffic and intersection scenarios.

139 The existing literature establishes a strong foundation for vehicle trajectory prediction using  
140 both traditional and deep learning methods. While LSTMs and transformer-based architectures  
141 have demonstrated promising results, most existing models continue to depend on external  
142 infrastructure-based data, limiting their applicability in mixed-traffic environments [16][17].  
143 More importantly, they often treat vehicle motion as a uniform process, without distinguishing  
144 between different maneuver types. In practice, however, intersection studies consistently show  
145 that left and right turns are far more error-prone than straight-through movements, both in terms  
146 of prediction drift and safety risk [18][19][20]. Forecasting models that ignore these maneuver-  
147 specific differences may achieve reasonable accuracy for straight trajectories but often show  
148 reduced reliability during turning—arguably the very moments when accurate prediction is most  
149 critical for avoiding conflicts.

150 In addition, many methods classify turns frame by frame, making them vulnerable to jitter,  
151 occlusion, or noise in tracking [21][22]. This often leads to unstable maneuver recognition,  
152 particularly during stationary periods or at the onset of a turn, thereby reducing the reliability of  
153 downstream prediction. While prior work has laid an important foundation for vehicle trajectory  
154 prediction, turning maneuvers remain especially challenging due to their variability and  
155 sensitivity to noise.

156 To complement these efforts, this study introduces a Turn-Aware LSTM that incorporates  
157 cumulative turning-angle encoding—a modest but practical refinement aimed at improving  
158 robustness for left and right turns while preserving accuracy for straight movements.

159 By explicitly representing left, right, and straight maneuvers through one-hot vectors, the  
160 model achieves more stable recognition and delivers improved trajectory prediction precisely  
161 where conventional models tend to degrade: during turning maneuvers and stationary phases at  
162 intersections.

163

### 164 **3. Methodology**

165 Traffic behavior detection plays a critical role in transportation research, particularly in the  
166 field of vehicle trajectory prediction. Traditional methods rely on trajectory analysis, using  
167 classical machine learning techniques such as Fuzzy C-Means (FCM) and Support Vector  
168 Machines (SVM) for classification. However, these methods struggle with feature robustness and  
169 scalability, particularly in dynamic traffic conditions. Recent advances in deep learning,  
170 particularly Long Short-Term Memory (LSTM) networks, have significantly improved the  
171 accuracy of trajectory prediction by modeling sequential dependencies in vehicle movement data.

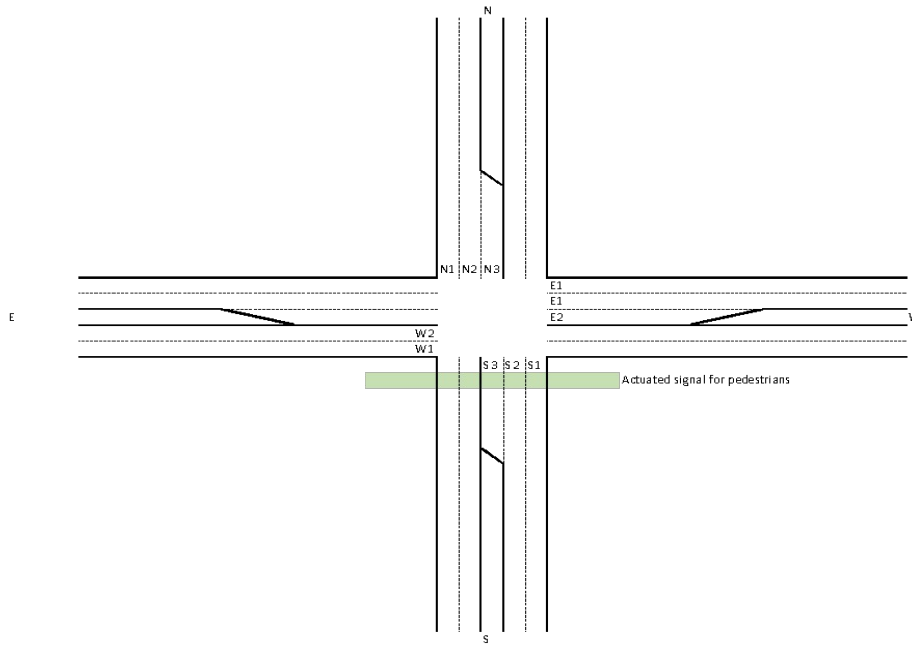
172 While existing LSTM-based models have demonstrated high accuracy in specific scenarios,  
173 they often fail to incorporate essential contextual features such as lane-specific functions and  
174 turning behaviors, which are critical for predicting vehicle movements in complex intersection  
175 environments.

176 To address these limitations, this study introduces a Turn-Aware LSTM model that explicitly  
177 encodes maneuver types (straight, left turn, right turn) alongside kinematic trajectory features.  
178 This design enables the model to learn differentiated motion dynamics across maneuvers, thereby  
179 improving prediction accuracy in exactly the situations where conventional models degrade.

180 The proposed methodology consists of five main components: data collection and  
181 preprocessing, vehicle detection and tracking, trajectory forecasting, turning behavior recognition  
182 and Turn-Aware LSTM. To ensure consistent scaling and facilitate model convergence, all  
183 numerical features were normalized before being fed into the Turn-Aware LSTM.

### 184 3.1 Data collection and preprocessing

185 As shown in Fig. 1, the study site is a four-arm signalized intersection in Châteauguay,  
186 Montreal. The layout includes two westbound lanes (W1–W2), three eastbound lanes (E1–E3),  
187 three southbound lanes (S1–S3), and three northbound lanes (N1–N3). The intersection design  
188 provides dedicated turning lanes that are clearly separated from through lanes under signal  
189 control. This configuration makes the site suitable for isolating turning maneuvers in the collected  
190 vehicle trajectories. Data were recorded on December 7th and 8th, 2020, during both peak and  
191 off-peak periods to capture diverse traffic conditions. The choice of this location reflects the  
192 study's focus on turning maneuvers, as the intersection's lane geometry—with dedicated turning  
193 lanes under signal control—provides a clear setting for examining how turning behavior can be  
194 explicitly modeled in trajectory forecasting.



195  
196  
197

*Fig. 1 - Layout of the four-arm signalized intersection in Châteauguay, Montreal, QC*

198  
199  
200  
201  
202  
203  
204

Fig. 2 presents the temporal distribution of traffic during the data collection period, reflecting the peak-hour congestion observed at the study site. The dataset comprises vehicles classified into passenger vehicles, trucks, and buses, each labelled with distinct identifiers for subsequent tracking. Video recordings were captured in 4K resolution at 30 fps, ensuring high-fidelity motion analysis.

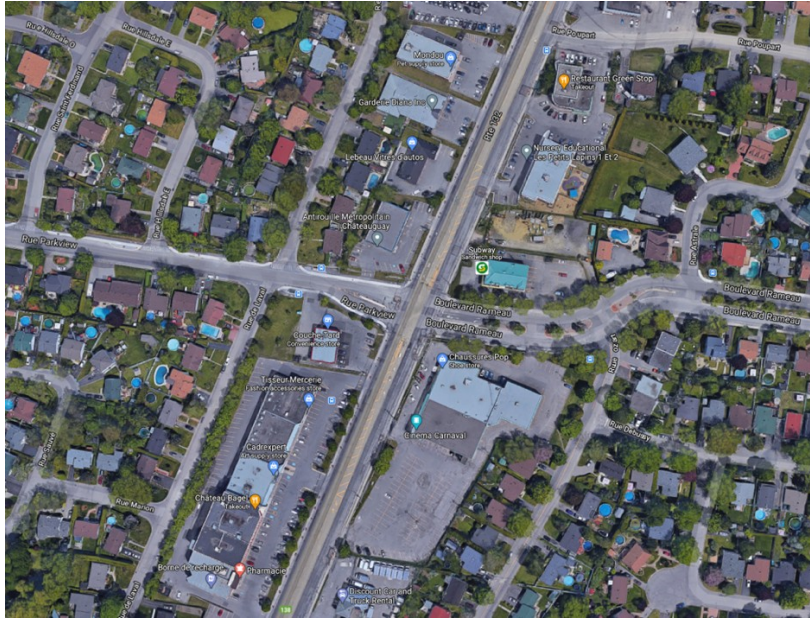


Fig. 2 - Aerial view of the study area in Châteauguay QC

205  
206  
207

208

209

210

211

212

213

214

215

216

217

Fig. 3 illustrates the UAV’s position at an altitude of approximately 80 meters above the intersection, which served as the basis for pixel-to-distance calibration. The altitude was programmatically fixed and remained stable throughout data collection. The main source of variability came from minor lateral drift or tilt caused by wind or GPS fluctuations. At this elevation, each pixel corresponded to about 3.5 meters, providing a critical conversion parameter for vehicle trajectory computation. To mitigate distortions, a Fourier–Mellin transform (FMT) was applied for video stabilization, correcting translational, rotational, and small-scale deviations across frames. This ensured reliable trajectory extraction, although residual perspective errors may persist at the image periphery, a limitation acknowledged in Section 5.

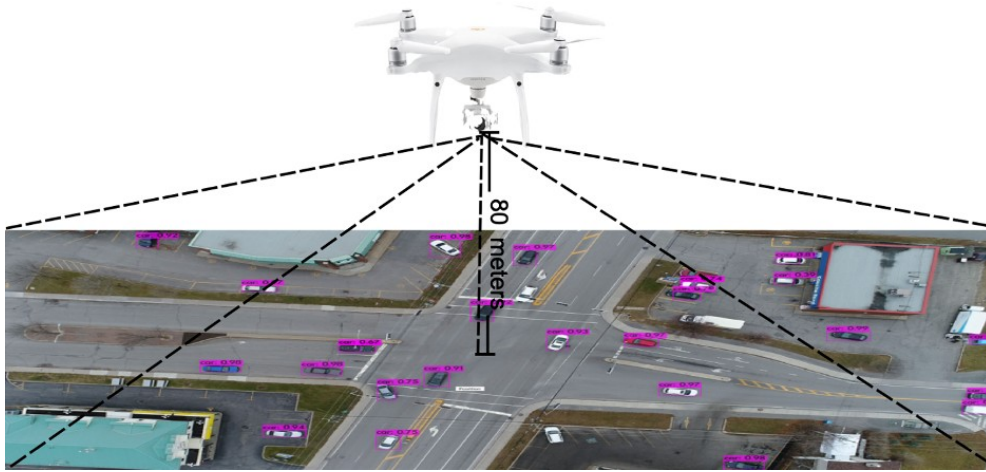


Fig. 3 - Drone positioned 80 meters above the intersection

218  
219  
220

221

222

To improve the consistency of trajectory extraction, a Fourier-Mellin transform was applied for video stabilization, mitigating translational and rotational deviations caused by UAV movement. This method effectively corrects distortions in video frames, ensuring continuous and reliable vehicle trajectories.

226

227

228

The Fourier-Mellin transform (FMT) leverages the Fourier rotation and similarity theorems to convert rotation and scaling into translations in log-polar space. Suppose two frames are related by translation and rotation, the transformation can be expressed as Equation (1)

229

$$f_2(x, y) = f_1(x \cos \theta + y \sin \theta - t_x, -x \sin \theta + y \cos \theta - t_y) \quad (1)$$

230

where:

231

•  $\theta$  is the rotation angle,

232

•  $t_x$  and  $t_y$  are translations in the  $x$  and  $y$  directions, respectively.

233

This transformation allows for effective compensation of rotation and scaling changes between consecutive frames, ensuring that detected vehicle trajectories remain continuous and unaffected by UAV movements.

235

236

237

To formally define the Fourier-Mellin transform of a function, we use Equation (2):

238

$$M_f(u, v) = \frac{1}{2} \int_0^{\infty} \int_0^{2\pi} f(r, \theta) r^{-ju} e^{-jv\theta} d\theta dr \quad (2)$$

239

where:

240

•  $u$  and  $r$  are the Mellin transform parameters,

241 •  $v$  and  $\theta$  are the Fourier transform parameters.

242 This transformation remaps the Fourier-transformed frame into log-polar coordinates,  
243 allowing rotation and scaling to be expressed as simple translations. By applying this correction,  
244 rotational and scaling misalignments in UAV video frames are eliminated, resulting in stabilized  
245 sequences that accurately reflect real-world vehicle movements.

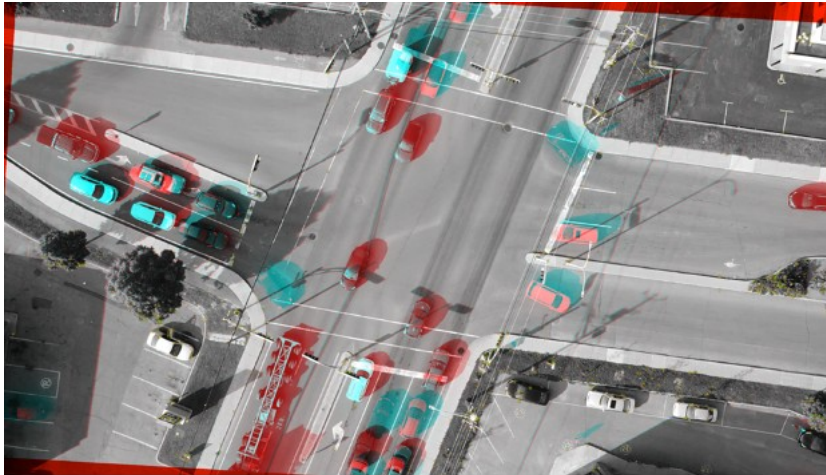
246 Fig. 4 illustrates the video frames before and after the Fourier-Mellin transform, highlighting  
247 the reduction in rotation and scaling effects. As seen in Fig. 5, color composite analysis visually  
248 confirms the improved alignment across successive frames.  
249



250  
251  
252

*Fig. 4 - Comparison of Original vs. Stabilized Frames (Fourier-Mellin Transform)*

253



254  
255  
256

*Fig. 5 - Frame Alignment via Color Composite Analysis*

257 Additionally, background subtraction techniques were employed to filter out static objects,  
258 reducing noise and enhancing the accuracy of subsequent vehicle detection and tracking.

260  
261 *3.2 Vehicle detection and tracking*  
262

263 For object detection, YOLOv8 was employed due to its high precision in urban environments.  
 264 The model was retrained on a custom dataset consisting of 18,000 labeled images to adapt to site-  
 265 specific vehicle characteristics. Labeling was conducted using Open Labeling, assigning unique  
 266 class identifiers (0 to 4) to different vehicle types (passenger cars, buses, and trucks). Given the  
 267 frequent presence of stationary vehicles at intersections, dataset redundancy was minimized by  
 268 selecting frames at 150-frame intervals, ensuring a balanced dataset. To further mitigate class  
 269 imbalance, data augmentation techniques were applied, including rotation, cropping, scaling, and  
 270 flipping, thereby improving the model's robustness in detecting underrepresented turning  
 271 behaviors.

272 Vehicle trajectories were extracted using Deep SORT, which assigns unique tracking IDs  
 273 across frames based on detections from YOLOv8. Each detected vehicle was represented by its  
 274 bounding box parameters  $(x_{center}, y_{center})$ , width, height, confidence score, and class label. Non-  
 275 Maximum Suppression (NMS) was applied to remove redundant detections using the Intersection  
 276 over Union (IoU), as Equation (3):  
 277

$$IoU(B_i, B_j) = \frac{\text{Area}(B_i \cap B_j)}{\text{Area}(B_i \cup B_j)} \quad (3)$$

278 where overlapping bounding boxes exceeding a threshold  $\theta$  were suppressed to maintain  
 279 detection accuracy.

### 281 3.3 Trajectory forecasting

282 Following vehicle trajectory extraction, a data cleaning pipeline was implemented to remove  
 283 outliers and interpolate missing detections. The comprehensive end-to-end workflow, from raw  
 284 data collection to the final LSTM-based forecasting, is summarized in Figure 6.  
 285  
 286  
 287  
 288

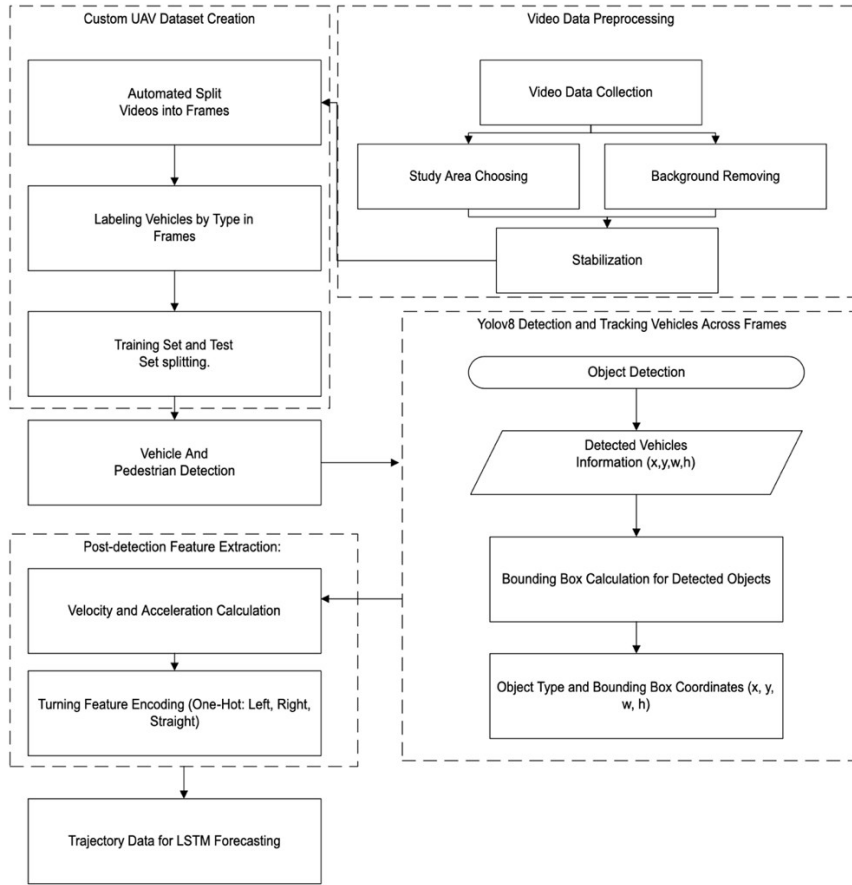


Fig. 6 - End-to-End Vehicle Trajectory Forecasting Model

After detection, vehicle velocities were computed using finite differences as Equation (4):

$$v_{x,t} = \frac{x_t - x_{t-1}}{\Delta t}, v_{y,t} = \frac{y_t - y_{t-1}}{\Delta t} \quad (4)$$

and acceleration components were estimated as Equation (5):

$$a_{x,t} = \frac{v_{x,t} - v_{x,t-1}}{\Delta t}, a_{y,t} = \frac{v_{y,t} - v_{y,t-1}}{\Delta t} \quad (5)$$

where  $\Delta t$  represents the time interval between frames. To ensure smooth and consistent velocity and acceleration estimates, a sliding window approach was applied to reduce

301 fluctuations. Additionally, forward and backward interpolation was used to handle missing  
302 detections, ensuring seamless trajectory continuity.

303 To reduce noise, a Savitzky-Golay filter was applied separately to the x and y coordinates,  
304 preserving motion dynamics while smoothing trajectories over a sliding window. The Savitzky-  
305 Golay filter operates by fitting a polynomial of degree  $k$  over a window of  $2m+1$  points for each  
306 coordinate, producing smoothed values  $x_i^{\text{smooth}}$  and  $y_i^{\text{smooth}}$ , as shown in Equation (6) and  
307 Equation (7).  
308

$$x_i^{\text{smooth}} = \sum_{j=-m}^m c_j x_{i+j} \quad (6)$$

309

$$y_i^{\text{smooth}} = \sum_{j=-m}^m c_j y_{i+j} \quad (7)$$

310

### 311 3.4 Turning behavior recognition

312 After trajectory preprocessing, turning behaviors were extracted and encoded to capture lane-  
313 change and maneuvering actions, which are essential for accurate vehicle trajectory forecasting.

314 The cumulative turning angle over each 1-second window was used to classify turning  
315 behavior as left, right, or straight.

316 To capture turning behaviors, an instantaneous direction angle was calculated using Equation  
317 (8):  
318

$$\phi_t = \text{atan2}(v_{y,t}, v_{x,t}) \quad (8)$$

319

320 Where  $v_{x,t}$  and  $v_{y,t}$  represent the velocity components. The angular change  $\Delta\phi_t$  between  
321 consecutive frames was then computed as Equation (9):  
322

$$\Delta\phi_t = \phi_t - \phi_{t-1} \quad (9)$$

323

324 A turning threshold of  $\Theta = 10^\circ$  (0.1745 rad) was adopted to classify maneuvers into left,  
325 right, and straight categories. Heading-change thresholds are widely used in trajectory  
326 segmentation, where turns are identified once cumulative direction changes exceed a predefined  
327 angle [23][24][25]. Prior work shows that thresholds in the range of  $5^\circ$ – $15^\circ$  are commonly applied  
328 to distinguish between lane-keeping and turning behavior, although the exact value depends on  
329 data resolution and noise characteristics. To verify robustness, we conducted a sensitivity analysis  
330 across three thresholds of  $5^\circ$ ,  $10^\circ$ , and  $15^\circ$ , and trajectory-level accuracy remained stable at  $\sim 83\%$   
331 across all settings.  
332  
333

Tab. 1 Sensitivity analysis results across three thresholds

Threshold (°)	Traj Overall	Left Acc	Straight Acc	Right Acc	Curve Recall	Straight FP	Onset Delay	Label Flips	Tracks Evaluated
------------------	-----------------	-------------	-----------------	--------------	-----------------	----------------	----------------	----------------	---------------------

	Acc						(s)	/100f	
5	0.835	0.807	0.874	0.833	0.203	0.44	0.0	21.08	260
10	0.835	0.807	0.874	0.833	0.2	0.439	0.0	20.96	260
15	0.835	0.807	0.874	0.833	0.197	0.439	0.0	20.86	260

334

335

336

337

338

339

340

341

This stability supports the adoption of  $10^\circ$  as a balanced threshold: small enough to detect true turning maneuvers, yet conservative against noise in frame-to-frame heading fluctuations. Based on this analysis, we operationalized the  $10^\circ$  rule at the frame level. At each time step  $t$ , the instantaneous direction angle  $\phi_t$  was compared against the threshold to assign a preliminary label of left, right, or straight, as shown in Equation (10):

$$m_t = \hat{i} \quad (10)$$

342

343

344

345

346

347

To mitigate noise at the frame level, the maneuver type of each trajectory was determined through aggregation rather than relying on instantaneous labels. Specifically, we applied a majority-vote strategy over the tail segment of the trajectory and required a minimum number of consecutive frames to confirm a turning event. This design ensures sensitivity to the onset of a turn while avoiding spurious fluctuations that may occur during short stops or tracking jitter.

348

349

350

351

352

353

Because LSTM models require numerical input, maneuver categories were encoded using a one-hot representation. This choice avoids introducing artificial ordinal relationships among the three classes (left, right, straight) and ensures that each maneuver is treated as an independent behavioral mode. The encoded features were then concatenated with the kinematic states and passed into the trajectory forecasting model, providing the LSTM with both motion history and maneuver context.

354

355

The final feature vector at each time step  $t$  was structured as Equation (11):

$$u_t = [x_t, y_t, v_{x,t}, v_{y,t}, a_{x,t}, a_{y,t}, m_{t,1}, m_{t,2}, m_{t,3}] \quad (11)$$

356

357

358

359

where  $m_{t,1}, m_{t,2}, \wedge m_{t,3}$  corresponded to the one-hot encoded turning classifications. The full input matrix for a vehicle's trajectory sequence was as Equation (12):

$$U_i = [u_{t_1}, u_{t_2}, \dots, u_{t_n}] \quad (12)$$

360

361

362

363

364

365

366

367

368

369

370

where  $n$  represents the number of time steps in the observation window.

Before feeding the trajectories into the prediction model, we performed consistency checks and normalization to ensure that the input data reflected physically plausible vehicle motion. This step was necessary because raw UAV-tracked trajectories can contain noise, missing detections, or unrealistic fluctuations. To address these issues, we applied the following procedures:

First, we identified and corrected implausible motion artifacts such as sudden position jumps, abrupt heading changes, and excessive acceleration spikes. Missing detections were handled by interpolation, either by propagating valid past or future values or by linear interpolation when both sides were available. After filling gaps, trajectories were resampled to the original frame rate of 30 fps to provide the temporal resolution required for sequential modeling.

371 Because frame-level turning cues are often noisy, turning-behavior encoding was performed  
372 on down-sampled one-second intervals to smooth jitter, and subsequently up-sampled back to 30  
373 fps for synchronization. Finally, all numerical features (positions, velocities, accelerations) were  
374 normalized with respect to their maximum observed values to facilitate model convergence and  
375 comparability across trajectories.

376 With preprocessed and normalized features in place, we proceeded to the Turn-Aware LSTM  
377 architecture, which integrates these inputs into an encoder–decoder framework for sequence-to-  
378 sequence trajectory forecasting.

### 379 3.5 Turn-Aware LSTM

381 The proposed predictor utilizes an encoder–decoder LSTM architecture for sequence-to-  
382 sequence trajectory forecasting. The encoder comprises a stacked two-layer LSTM with a hidden  
383 size of 128 units to process the observed sequence and compress temporal dependencies into final  
384 hidden and cell states. Initialized with these states, the decoder autoregressively generates the  
385 future trajectory for the specified prediction horizon. At each decoding step, a linear projection  
386 maps the hidden state to 2D coordinates  $x$  and  $y$ . Training employs the Mean Squared Error loss  
387 and the Adam optimizer with a learning rate of 0.001. To enhance generalization, an early  
388 stopping mechanism is implemented if the validation loss remains stagnant for ten consecutive  
389 epochs.

## 390 4. Experiment

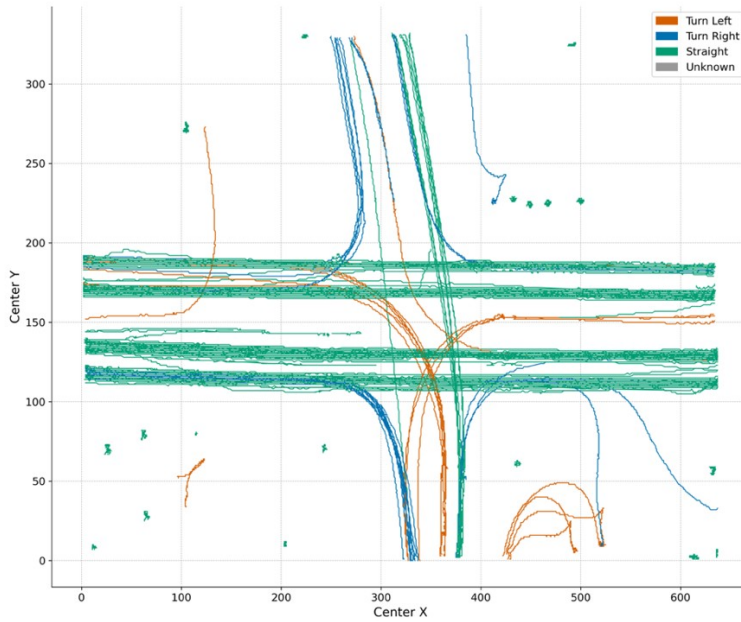
### 392 4.1 Experimental Setup

393 The dataset was divided into training (70%), validation (15%), and test (15%) sets, ensuring  
394 trajectories from the same vehicle remained within a single subset. Performance was evaluated at  
395 horizons of 1.0 s, 2.0 s, and 3.0 s (30, 60, and 90 frames). The Turn-Aware LSTM was compared  
396 against three baselines: (i) a physics-based Constant Velocity (CV) model; (ii) a conventional  
397 Vanilla LSTM; and (iii) a Tiny Transformer representing the state-of-the-art. This setup isolates  
398 the targeted accuracy gains of explicit maneuver encoding during turning maneuvers.

### 400 4.2 Feature Engineering and Visualization

401 To illustrate the impact of maneuver encoding, Figure 7 presents vehicle trajectories  
402 categorized into left turns, right turns, and straight movements. All trajectories were pre-  
403 processed with  $y$ -coordinate inversion to maintain consistency with the tracking system. These  
404 encoded behaviours serve as essential inputs, enabling the LSTM to capture complex  
405 maneuvering patterns and improve anticipation of vehicle movements compared to raw trajectory  
406 data.

407  
408  
409



410  
411  
412  
413

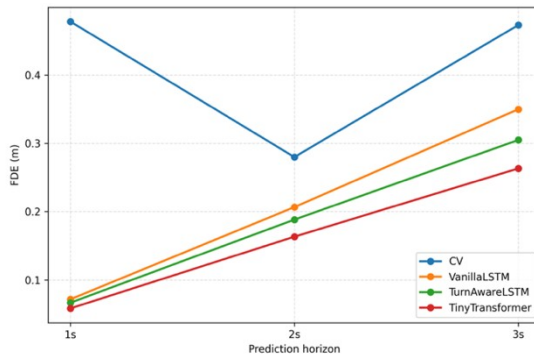
Fig. 7 Vehicle trajectories after turning feature encoding, categorized into left turns, right turns, and straight movements.

414  
415

### 4.3 Comparative Analysis across Models and Maneuvers

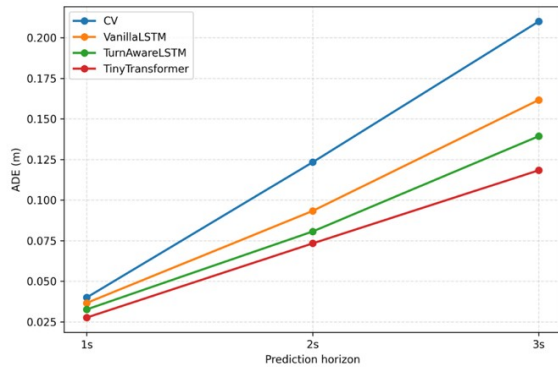
416  
417  
418  
419  
420  
421  
422

As illustrated in Figure 8 and Figure 9 prediction errors increase with longer horizons due to accumulated uncertainty. The Tiny Transformer achieves the lowest overall Average Displacement Error (ADE) and Final Displacement Error (FDE), while the Turn-Aware LSTM consistently outperforms the Vanilla LSTM, particularly at the 3s horizon (0.30 m vs. 0.35 m FDE). The CV baseline exhibits unstable and significantly higher errors across all metrics, confirming the necessity of sequence modelling for intersection dynamics.



423  
424

Fig. 8 Average FDE across all maneuvers over different prediction horizons



425  
426

Fig. 9 Average ADE across all maneuvers over different prediction horizons

427  
428  
429  
430  
431  
432  
433  
434  
435

The targeted benefit of turn encoding is highlighted in Figure 10 and Figure 11. For right turns, the Turn-Aware LSTM cuts the extreme drift produced by the CV model almost in half, reaching ~0.42 m at 3 s. For left turns, the model reduces error from ~0.35 m (Vanilla LSTM) to ~0.28 m at 3 s, validating the use of maneuver-aware features in curbing curvature misestimation. Performance on straight motion remains comparable across all learning-based models, confirming that turn features do not interfere with trivial forward motion. Inference times on an RTX 4090 were ~2.5 ms per trajectory, confirming the model's suitability for real-time deployment.

436  
437

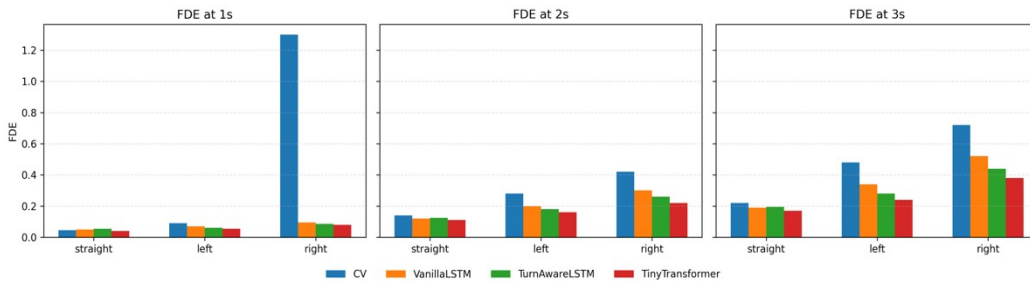


Fig. 10 FDE across all maneuvers over different prediction horizons

438  
439

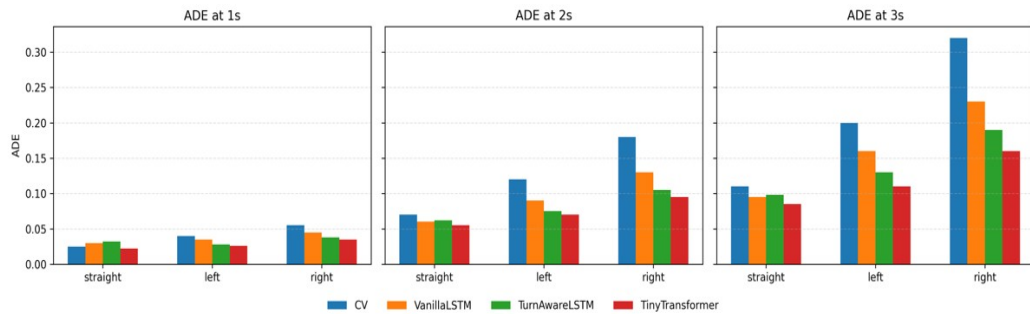


Fig. 11 ADE across all maneuvers over different prediction horizons

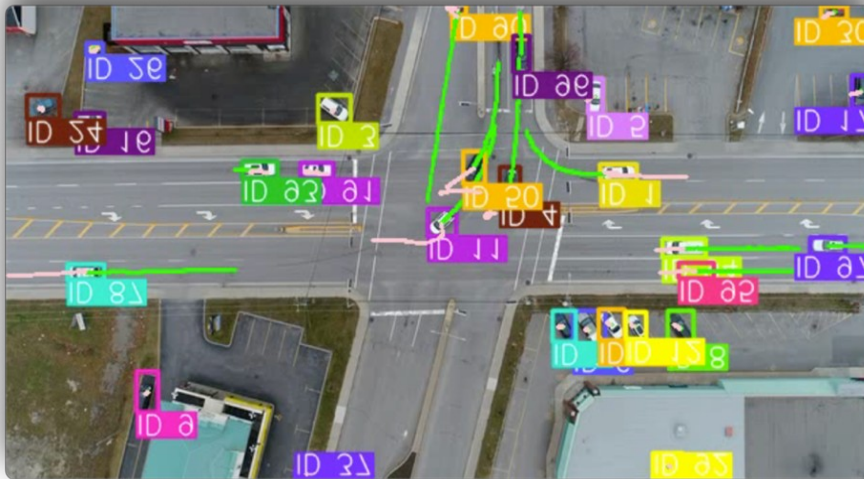
440 In addition to accuracy, we also evaluated computational efficiency. On an RTX 4090 GPU,  
 441 inference times were  $\sim 2.5$  ms per trajectory for the Turn-Aware LSTM,  $\sim 2.3$  ms for Vanilla  
 442 LSTM, and  $\sim 4.8$  ms for Tiny Transformer, while the CV baseline was nearly instantaneous ( $< 1$   
 443 ms). This confirms that the proposed turn-aware encoding introduces only minimal overhead  
 444 compared to a standard LSTM, while remaining well within the latency requirements for real-time  
 445 deployment.

#### 447 4.4 Experiment Discussion

448 Turning maneuvers remain the most challenging to predict due to detection jitter, which can  
 449 cause spurious angular fluctuations during stationary periods [26]. Our experimental analysis  
 450 (formerly illustrated via frame-level labelling) revealed that vehicles waiting at red lights could be  
 451 misclassified as executing rapid turns in consecutive frames due to minor tracking noise. To  
 452 address this, we adopted a cumulative turning angle strategy that aggregates directional changes  
 453 over a 1-second window. This approach successfully smooths frame-level jitter and ensures that  
 454 the reported performance gains, such as the 20% FDE reduction for left turns, reflect genuine  
 455 improvements in trajectory prediction rather than artifacts of noisy labelling.

456 Figure 12 provides a representative snapshot of the real-time pipeline, confirming the model's  
 457 robustness. For instance, vehicles executing left and right turns (e.g., IDs 11, 50, and 1) follow the  
 458 ground truth paths closely without the curvature drift typical of vanilla LSTMs. Crucially, the  
 459 cumulative-angle method correctly identifies stationary vehicles (e.g., IDs 24 and 26) as stopped,  
 460 maintaining stable forecasts even under detection fluctuations. With a minimal computational  
 461 overhead of  $\sim 2.5$  ms per trajectory, the Turn-Aware LSTM demonstrates a practical balance  
 462 between accuracy and real-time efficiency.

463



464

465

466

Fig. 12 Forecasted and ground truth trajectories visualization

467  
468**5. Conclusion**

469 This study demonstrates that explicitly encoding turning behaviours via cumulative heading  
470 changes improves vehicle trajectory forecasting, reducing FDE by 15–20% for turning maneuvers  
471 compared to a vanilla LSTM. The model’s lightweight design (~2.5 ms inference) makes it  
472 suitable for real-time autonomous driving and proactive traffic safety management without  
473 reliance on GPS or detailed maps. While the Tiny Transformer achieves lower long-horizon  
474 errors, the Turn-Aware LSTM provides targeted improvements where they matter most—at turns.  
475 Future research will focus on integrating maneuver encoding into graph-based interaction models  
476 and validating the framework on larger datasets like Waymo to improve robustness in high-  
477 density, multi-agent traffic environments.

478  
479**5.1. Data Availability Statement**

480 The processed trajectory datasets, maneuver annotations, and model code are available at the  
481 following repository: [https://github.com/Jynxzzz/Turn-Aware-LSTM\\_SUPP](https://github.com/Jynxzzz/Turn-Aware-LSTM_SUPP). Due to privacy and  
482 data-sharing restrictions, raw video data cannot be publicly released.

483  
484**6. Acknowledgments**

485 This work was funded and supported by Ericsson - Global Artificial Intelligence Accelerator  
486 AI Hub Canada in Montréal through the Mitacs Accelerate Program. The authors would like to  
487 express their gratitude for the valuable comments and collaboration provided by GAIA Montréal,  
488 as well as the support from all collaborators involved in this study.

489  
490**7. References**

- 491 1. Tilg, G., Krause, S. and Bogenberger, K. (2021). 3. automatisierte Fahrzeuge, vernetzte Fahrzeuge,  
492 Managed Lanes, Kapazität. 2021.
- 493 2. Yan, X., He, J., Wu, G., Sun, S., Wang, C., Fang, Z. and Changjian, Z. (2024). 2. Driving risk  
494 identification of urban arterial and collector roads based on multi-scale data. *Accident Analysis &*  
495 *Prevention*.
- 496 3. Liao, H., Li, Z., Wang, C., Shen, H., Liao, D., Wang, B., ... Xu, C.-Z. (2024). MFTraj: Map-Free,  
497 Behavior-Driven Trajectory Prediction for Autonomous Driving.
- 498 4. Lin, L., Li, W., Bi, H. and Qin, L. (2021). Vehicle Trajectory Prediction Using LSTMs with Spatial-  
499 Temporal Attention Mechanisms. *IEEE Intelligent Transportation Systems Magazine*, pp. 0–0.
- 500 5. Wang, J., Liu, K. and Li, H. (2024). LSTM-based graph attention network for vehicle trajectory  
501 prediction. *Computer Networks*.
- 502 6. Saini, R., Kumar, P., Roy, P. P. and Dogra, D. P. (2017). An efficient approach for trajectory  
503 classification using FCM and SVM. July 2017.
- 504 7. Yao, D., Zhang, C., Zhu, Z., Huang, J. and Bi, J. (2017). Trajectory clustering via deep representation  
505 learning. May 2017.
- 506 8. Choong, M., Angeline, L., Chin, R., Yeo, K. B. and Teo, K. (2017). Modeling of vehicle trajectory  
507 clustering based on LCSS for traffic pattern extraction. October 1, 2017.
- 508 9. Hochreiter, S. and Schmidhuber, J. (1997). Long Short-Term Memory. *Neural Computation*, 9, n. 8,  
509 pp. 1735–1780.
- 510 10. How, D. N. T., Loo, C. K. and Sahari, K. S. M. (2016). Behavior recognition for humanoid robots  
511 using long short-term memory. *International Journal of Advanced Robotic Systems*, 13, n. 6, pp.  
512 1729881416663369.

- 513 11. Morton, J., Wheeler, T. A. and Kochenderfer, M. J. (2017). Analysis of Recurrent Neural Networks  
514 for Probabilistic Modeling of Driver Behavior. *IEEE Transactions on Intelligent Transportation*  
515 *Systems*, 18, n. 5, pp. 1289–1298.
- 516 12. Ding, L., Fang, W., Luo, H., Love, P. E. D., Zhong, B. and Ouyang, X. (2018). A deep hybrid  
517 learning model to detect unsafe behavior: Integrating convolution neural networks and long short-  
518 term memory. *Automation in Construction*, 86, pp. 118–124.
- 519 13. Yang, C. and Pei, Z. (2023). Long-Short Term Spatio-Temporal Aggregation for Trajectory  
520 Prediction. *IEEE Transactions on Intelligent Transportation Systems*, 24, pp. 4114–4126.
- 521 14. Varghese, R. and M, S. (2024). YOLOv8: A Novel Object Detection Algorithm with Enhanced  
522 Performance and Robustness. 2024.
- 523 15. Coifman, B. and Li, L. (2017). A critical evaluation of the Next Generation Simulation (NGSIM)  
524 vehicle trajectory dataset. *Transportation Research Part B: Methodological*, 105, pp. 362–377.
- 525 16. Geng, M., Li, J., Xia, Y. and Chen, X. (Michael). (2023). A physics-informed Transformer model for  
526 vehicle trajectory prediction on highways. *Transportation Research Part C: Emerging Technologies*,  
527 154, pp. 104272.
- 528 17. Ying, J. and Feng, Y. (2024). Infrastructure-Assisted cooperative driving and intersection  
529 management in mixed traffic conditions. *Transportation Research Part C: Emerging Technologies*,  
530 158, pp. 104443.
- 531 18. Ghanim, M. and Shaaban, K. (2018). Estimating Turning Movements at Signalized Intersections  
532 Using Artificial Neural Networks. *IEEE Transactions on Intelligent Transportation Systems*, PP, pp.  
533 1–9.
- 534 19. Zhang, S., Abdel-Aty, M., Cai, Q., Li, P. and Ugan, J. (2020). Prediction of pedestrian-vehicle  
535 conflicts at signalized intersections based on long short-term memory neural network. *Accident*  
536 *Analysis & Prevention*, 148, pp. 105799.
- 537 20. Schulz, J., Hubmann, C., Löchner, J. and Burschka, D. (2018). Interaction-Aware Probabilistic  
538 Behavior Prediction in Urban Environments. arXiv.
- 539 21. Gulzar, M., Muhammad, Y. and Muhammad, N. (2021). A Survey on Motion Prediction of  
540 Pedestrians and Vehicles for Autonomous Driving. *IEEE Access*, PP, pp. 1–1.
- 541 22. Hartjen, L., Philipp, R., Schuldt, F., Howar, F. and Friedrich, B. (2019). Classification of Driving  
542 Maneuvers in Urban Traffic for Parametrization of Test Scenarios. November 22, 2019.
- 543 23. Aboah, A., Adu-Gyamfi, Y., Gursoy, S. V., Merickel, J., Rizzo, M. and Sharma, A. (2023). Driver  
544 Maneuver Detection and Analysis Using Time Series Segmentation and Classification. *Journal of*  
545 *transportation engineering. Part A, Systems*, 149, n. 3, pp. 7312.
- 546 24. Phuyal, B. P. (2002). Turn detection algorithm for vehicle positioning.
- 547 25. Wan, Z., Li, L., Yu, H. and Yang, M. (2022). A Long Short-Term Memory-Based Approach for  
548 Detecting Turns and Generating Road Intersections from Vehicle Trajectories. *Sensors*, 22, n. 18, pp.  
549 6997.
- 550 26. Zhao, X., Wang, G., He, Z. and Jiang, H. (2022). A survey of moving object detection methods: A  
551 practical perspective. *Neurocomputing*, 503, pp. 28–48.
- 552